Int. J. of Thermodynamics
ISSN 1301-9724

Vol. 13 (No. 2), pp. 35-42, 2010
www.icatweb.org/ijot

Lamella / Rod Transformation as described by the Criterion of Minimum Entropy Production

W. S. Wołczyński*

Institute of Metallurgy and Materials Science, Polish Academy of Sciences,
Reymonta 25, 30 059 Kraków, Poland
nmwolczy@imim-pan.krakow.pl

Abstract

A general theory for the lamella ➔ rod transformation is presented. The analysis has been developed in two steps: first, taking into account the condition of minimum *Gibbs'* free energy, next, using the criterion of minimum entropy production together with the concept of marginal stability. The present theory provides a justification for theoretical determination of a threshold growth rate at which solidification begins to form a rod-like structure instead of a lamellar one. Additionally, the so-called operating range for transformation is justified by the oscillation between the trajectory of minimum entropy production and the trajectory of marginal stability. A model of the evolution of the mechanical equilibrium is introduced to satisfy some changes of the curvature of the solid / liquid interface with increasing growth rate. A consideration associated with the *Gibbs'* free energy allows to formulate a new criterion which predicts whether the lamellar structure is the stable form or a rod-like structure is the stable form (for a given phase diagram). An application of the criterion of minimum entropy production, together with a model of the instability of the solid/liquid interface (referred to as marginal stability), allows for determining a/ a trajectory at which a regular structure is forming and b/ a trajectory of marginal stability at which the maximum destabilization of the s/l interface of the non-faceted phase is observed together with the faceted phase branching.

Keywords: *Spacing oscillation, marginal stability, attractor, threshold rate for the lamella / rod transformation.*

1.Introduction

Many eutectic systems exhibit either a lamellar or rod-like structure depending on solidification conditions, Elliott (1977). Especially, growth rate plays a crucial role in the lamella / rod transformation. Some impurities are also involved in the transition, Steen and Hellawell (1975). The impurities change the specific surface free energies and finally modify a mechanical equilibrium at the triple point of the solid/liquid interface. However, according to the current model assumptions, the mechanical equilibrium varies with solidification conditions (growth rate) and no effect of impurities is observed. A given growth rate influences the crystal orientation. Some changes of the orientation from an initial state into a final one also give an effect on the lamella / rod transition, Figure 1.

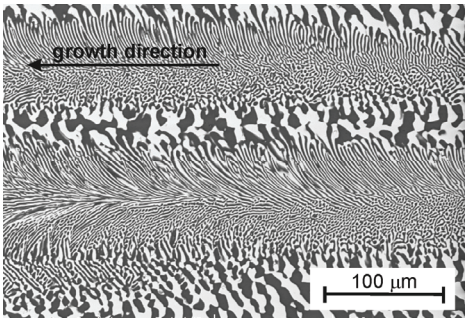

Figure 1. Transformation from a lamellar into a rod-like structure as observed during oriented growth of the eutectic cells; the Al - Al_2Cu system: v = 12 cm/h, G = 100 K/cm.

The theory developed by Jackson and Hunt (1966) has tried to predict the threshold rate at which transformation should occur.

The theory is based on the description of the solid / liquid interface undercooling which yields the inequality:

$$\frac{\left(a_\alpha^L/m_\alpha + a_\beta^L/\xi\, m_\beta\right)}{\left(a_\alpha^R/m_\alpha + a_\beta^R/\xi\, m_\beta\right)} > \frac{4E}{P^*}\frac{1}{(1+\xi)^{1.5}} \tag{1}$$

a/ with the undercooling defined for the lamellar growth,

$$(\Delta T_L^*)^2 = 4\, v\, m^2\, a^L\, Q^L \tag{1a}$$

b/ with the undercooling defined for the rod-like growth,

$$(\Delta T_R^*)^2 = 4\, v\, m^2\, a^R\, Q^R \tag{1b}$$

The discerning analysis shows that the above inequality is able to predict whether an eutectic alloy will only manifest a lamellar or rod-like structure. Thus, the inequality characterizes a given phase diagram. Eq. (1) cannot be applied to describe the lamella ➔ rod transformation.

For the isotropic solid-liquid interfacial free energies the l.h.s. of the considered equation is equal to one, Figure 2.

*Corresponding Author

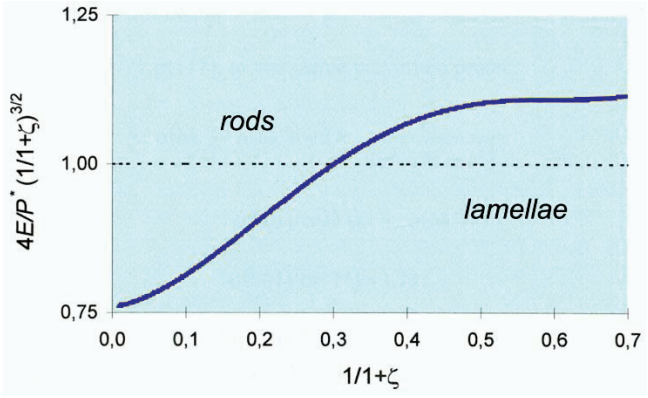

Figure 2. Prediction of an appearance of the rod-like or the lamellar structure, respectively (due to Eq. (1)).

Eq. (1) yields a result, according to which, when the following inequality is satisfied: $1/(1+\xi) < 0.32$, (for the assumed isotropy) then a rod-like structure is the stable form. This parameter is equal to 0.114 for the Al-Si system. Thus, the rod-like structure should be the stable form. Meanwhile, according to experimental observations a lamellar structure is the stable form instead of a rod-like structure. Moreover, the lamellar structure transforms into the rod-like structure at a critical growth rate named as the threshold growth rate.

It is evident that Eq. (1) is completely misleading. Therefore, a new condition for transformation based on the free energy calculation will be given in the current model. The threshold growth rate will also be determined for the Al-Si eutectic system by means of the current analysis. Additionally, the entropy production calculation will be performed to confirm the predictions given by the free energy analysis. An instability of the s/l interface of non-faceted phase will also be considered in order to show that the transformation occurs within a range of growth rates named as the so-called operating range for the transformation.

2. Thermodynamics of the eutectic solid/liquid interface

The thermodynamics of the s/l interface involves the calculation of the *Gibbs'* free energy for the considered Al-Si system which manifests an irregular structure within which regular structure areas exist. An effect of control parameters on the appearance of lamellar or rod-like structure within Al-Si eutectic alloy is well known due to experimental works, Toloui and Hellawell (1976) and Atasoy (1984).

It results from the experimental observations of both lamellar and rod-like structure formations that the threshold rate of solidification for lamella ➔ rod transformation is equal to 400 μm/s. The transformation is completed at the rate equal to about 700 μm/s. Both structures are visible within the operating range for the transformation, as revealed in Figure 3b, but the lamellar structure is obtainable below the threshold solidification rate, exclusively, as it is shown in Figure 3a.

The *Gibbs'* free energy formulas which are concerning the solid / liquid interface formation are as follows: a/ for the lamellar structure formation,

$$\Delta G_L^* = v\,\lambda\,Q_{C-W}^L + a_{C-W}^L\,\lambda^{-1} \qquad (2a)$$

b/ for the rod-like structure formation,

$$\Delta G_R^* = v\,R\,Q_{C-W}^R + a_{C-W}^R\,R^{-1} \qquad (2b)$$

Eq. (2a) was developed from Eq. (1a) by means of the transformation of the undercooling into the *Gibbs'* free energy. Also, Eq. (2b) was developed from Eq. (1b).

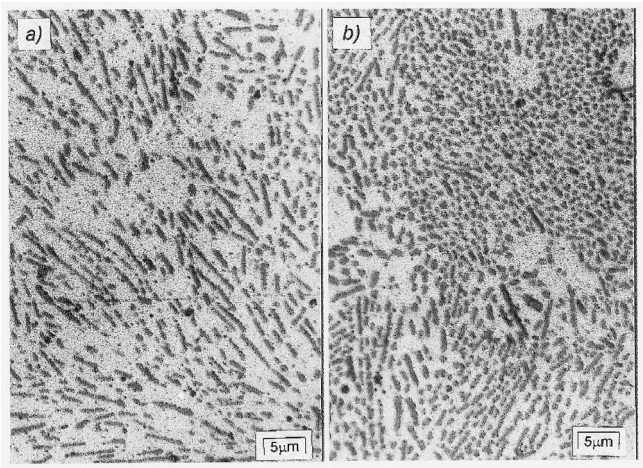

Figure 3. A cross-sectional morphology of a directionally solidifying Al-Si eutectic alloy, a/ for v = 370 μm/s and for G=100 K/cm, (lamellae exclusively); b/ for v=500 μm/s and G=40 K/cm, (lamellae + rods).

Some parameters used in Eqs. (2a)-(2b) are defined as:

$$Q_{C-W}^L = \left[m\,\left(L_\alpha\,\xi + L_\beta\right)/T_E\right]\left[P^*(1+\xi)\,N_0/(\xi\,D)\right] \qquad (3a)$$

$$Q_{C-W}^R = \left[m\,\left(L_\alpha\,\xi + L_\beta\right)/T_E\right]\left[4\,E\,N_0/(\xi\,D)\right] \qquad (3b)$$

$$a_{C-W}^L = m(1+\xi)\left[(\sigma_\alpha^L \sin\theta_\alpha^L)/m_\alpha + (\sigma_\beta^L \sin\theta_\beta^L)/(\xi\,m_\beta)\right] + \sigma_{\alpha-\beta}^L \qquad (4a)$$

$$a_{C-W}^R = 2\{m\sqrt{1+\xi}\left[(\sigma_\alpha^R \sin\theta_\alpha^R)/m_\alpha + \sigma_\beta^R \sin\theta_\beta^R/(\xi m_\beta)\right] + \sigma_{\alpha-\beta}^R/\sqrt{1+\xi}\} \qquad (4b)$$

with some additional parameters defined in Figure 4.

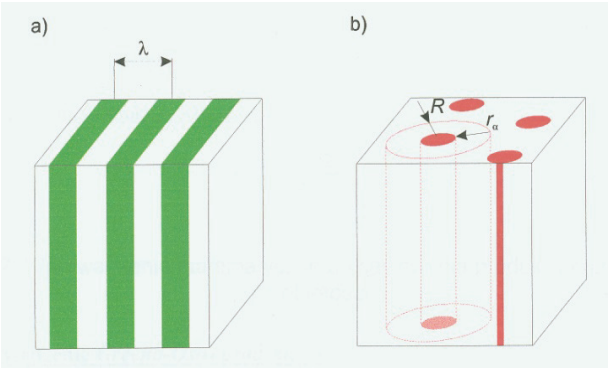

Figure 4. Some geometrical parameters which define both morphologies; a/ inter-lamellar spacing, λ within the regular lamellar structure, and b/ rod/(rod+matrix) radiuses within the regular rod-like structure.

Moreover, the following definitions are necessary to describe the morphologies of regular lamellar and rod-like eutectic:

$$\xi = S_\beta/S_\alpha \quad \text{with} \quad \lambda = 2\left(S_\alpha + S_\beta\right) \qquad (5a)$$

$$r_\alpha = 1/\sqrt{1+\xi} \quad \text{with} \quad R = r_\alpha + r_\beta \tag{5b}$$

Eq. (2) allows the development of the following inequality:

$$\frac{m\left(a_\alpha^L/m_\alpha + a_\beta^L/\xi\, m_\beta\right) + \sigma_{\alpha-\beta}^L/1+\xi}{m\left(a_\alpha^R/m_\alpha + a_\beta^R/\xi\, m_\beta\right) + \sigma_{\alpha-\beta}^R/1+\xi} > 4\frac{E}{P^*}\left(\frac{1}{1+\xi}\right)^{3/2} \tag{6}$$

Eq. (6) was developed in the same manner as Eq.(1) in the theory given by Jackson and Hunt (1966). It can also be used in the prediction of the stable form of the structure. A prediction obtained by means of Eq. (6) is similar to that which results from Eq. (1). So, the inequality cannot predict the lamella➔rod transformation in the Al-Si eutectic.

Therefore, the *Gibbs'* free energy, Eq. (2), was calculated by introducing the evolution of a mechanical equilibrium at the triple point of the solid / liquid interface, Figure 5.

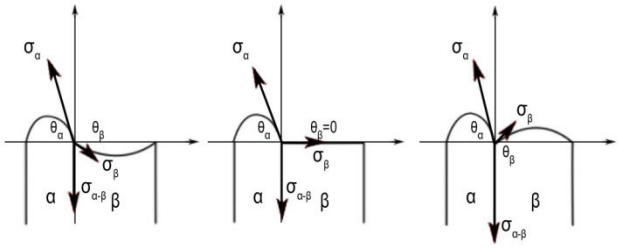

Figure 5. Typical curvatures of the solid/liquid interface of the regular eutectic and adequate mechanical equilibrium.

The mechanical equilibrium for both structure types is:

$$\sigma_\alpha^L \sin\theta_\alpha^L + \sigma_\beta^L \sin\theta_\beta^L - \sigma_{\alpha-\beta}^L = 0 \tag{7a}$$

$$\sigma_\alpha^R \sin\theta_\alpha^R + \sigma_\beta^R \sin\theta_\beta^R - \sigma_{\alpha-\beta}^R = 0 \tag{7b}$$

The *Gibbs'* free energy, Eq. (2), calculated for the three considered solidification rates, is shown in Figure 6.

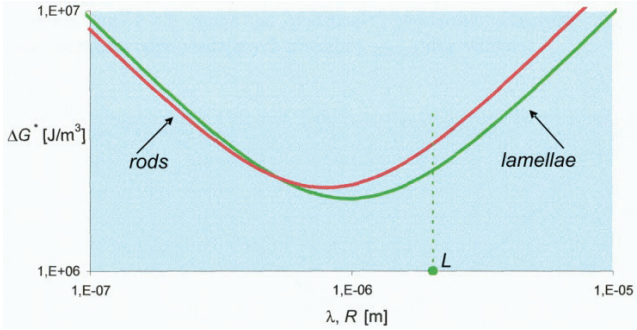

Figure 6a. Gibbs' free energy calculated for the formation of both structures at v=100 μm/s; dot L – denotes the localization of the average inter-lamellar spacing, $\bar{\lambda}$.

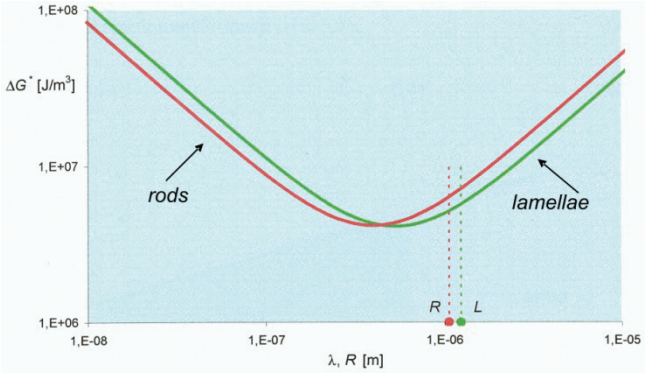

Figure 6b. Gibbs' free energy calculated for the formation of both structures at the threshold rate, v=400 μm/s; dot L – denotes the localization of the average inter-lamellar spacing, $\bar{\lambda}$ and dot R – denotes the localization of the average inter-rod spacing, $\bar{R}$.

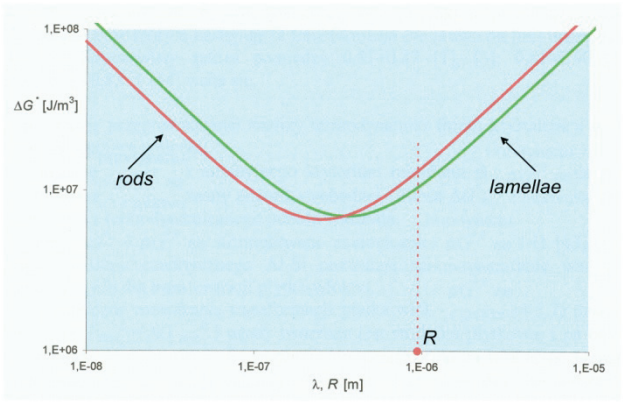

Figure 6c. Gibbs' free energy calculated for the formation of both structures at v=1000 μm/s; dot R – denotes the localization of the average inter-rod spacing, $\bar{R}$.

All the minima of the calculated *Gibbs'* free energy for all considered solidification rates are gathered in Figure 7.

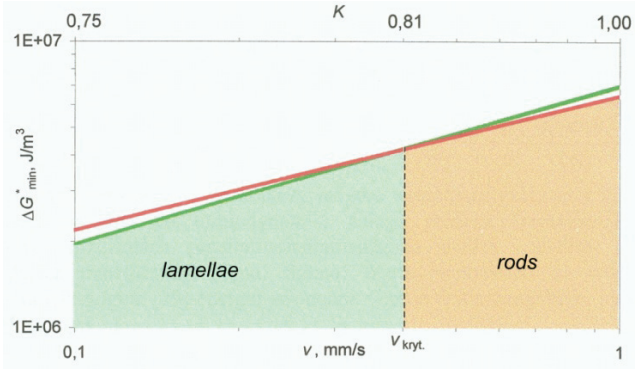

Figure 7. Gibbs' free energy minima calculated for lamellar and rod-like structures formation at the different solidification rates, typical for oriented growth of the Al-Si eutectic alloy; the critical growth rate, $v_{kryt.}$ for the lamella ➔ rod transformation results from the trajectories intersection; it is equal to the threshold rate, v = 400 μm/s.

According to the result of the *Gibbs'* free energy calculation this structure is a stable form which has its minimum situated lower. Thus, the calculation allows the determination of the threshold rate, when minima are at the same level, Figure 6b. The operating range is not yet described.

3. Thermodynamics of the whole solidification process

The thermodynamics of the whole solidification process involves a calculation of entropy production for the regular structure growth, Lesoult and Turpin (1969). The regular structure areas can be distinguished in a generally irregular structure of the Al-Si eutectic, Fisher and Kurz (1980).

The regular structure formation at steady-state should be described by the criterion of minimum entropy production. For that reason the entropy production, P_D was calculated assuming an isothermal solid/liquid interface.

$$P_D = \int_V \sigma_D \, dV \tag{8}$$

where the entropy production per unit time and unit volume formulated for constant temperature is as follows:

$$\sigma_D = D\, R^*\, \varepsilon \left(N_i(1-N_i)\right)^{-1} |grad.\, N_i|^2 \tag{9}$$

The entropy production, Eq. (9) was calculated for the mass transport associated with thermo-diffusion only, Glansdorff and Prigogine (1971), since the heat transfer was neglected. Also, it was necessary to introduce the solution to diffusion equation for steady state into the integral given by Eq. (8). Therefore, the solution to diffusion equation developed by Jackson and Hunt (1966) was used in the calculation of total entropy production for the considered structures formation. Finally, an average entropy production associated with the mass transport was calculated:

a/ for lamellar structure formation (regular lamellae within generally irregular morphology):

$$\bar{P}_D^L = W_1\, v\left(S_\alpha + S_\beta\right)^{-1} + W_2\, v\left(S_\alpha + S_\beta\right)^{-2} + W_3\, v^2 + W_4\, v^2\left(S_\alpha + S_\beta\right) + W_5\, v^3\left(S_\alpha + S_\beta\right)^2 \tag{10a}$$

b/ for rod-like structure formation (regular rods within generally irregular morphology):

$$\bar{P}_D^R = V_1\, v\left(r_\alpha + r_\beta\right)^{-1} + V_2\, v\left(r_\alpha + r_\beta\right)^{-2} + V_3\, v^2 + V_4\, v^2\left(r_\alpha + r_\beta\right) + V_5\, v^3\left(r_\alpha + r_\beta\right)^2 \tag{10b}$$

The volumes required in Eq. (8) are defined as follows:

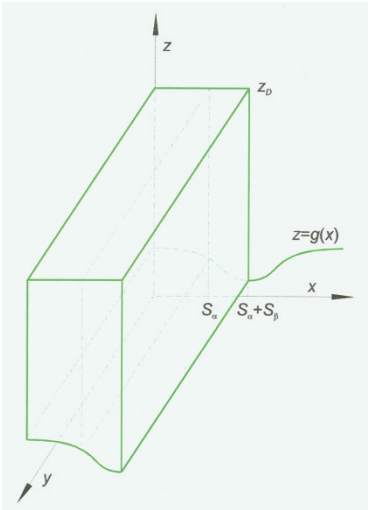

Figure 8a. Volume adequate for a lamellar growth, Eq.(8).

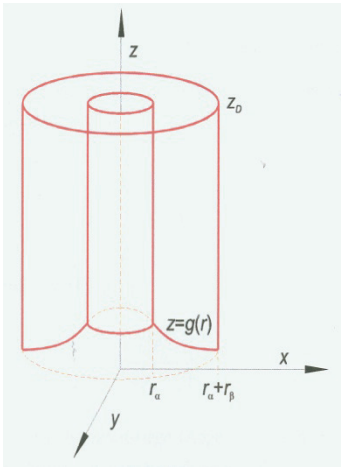

Figure 8b. Volume adequate for a rod-like growth, Eq.(8).

W_i and V_i , $i = 1, \ldots, 5$ - coefficients contain some material parameters that define both lamellar and rod-like structures formation, respectively, Wołczyński and Billia, (1996).

The structural spacing and co-ordinate system which moves with the s/l interface are shown in Figures (9a)-(9b).

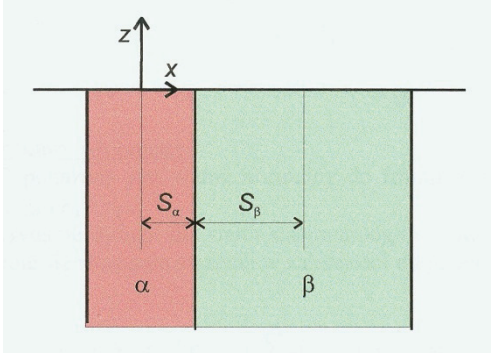

Figure 9a. Geometry and spacing of the lamellar structure.

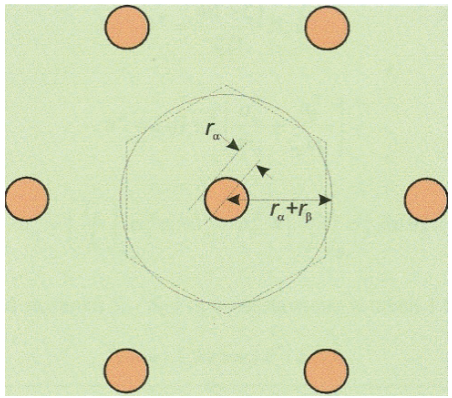

Figure 9b. Geometry and spacing of the rod-like structure.

A minimization of Eqs. (10a)-(10b) involves:
a/ for the formation of lamellar eutectic structure:

$$\partial \bar{P}_D^L / \partial\left(S_\alpha + S_\beta\right) = -W_1\, v\left(S_\alpha + S_\beta\right)^{-2} - 2\, W_2\, v\left(S_\alpha + S_\beta\right)^{-3} + 2\, W_5\, v^3\left(S_\alpha + S_\beta\right) = 0 \tag{11a}$$

b/ for the formation of rod-like eutectic structure:

$$\partial \bar{P}_D^R / \partial\left(r_\alpha + r_\beta\right) = -V_1\, v\left(r_\alpha + r_\beta\right)^{-2} - 2\, V_2\, v\left(r_\alpha + r_\beta\right)^{-3} + 2 V_5\, v^3\left(r_\alpha + r_\beta\right) = 0 \tag{11b}$$

The minima of the entropy production, for both types of structure, are gathered in Figure 10. The curves which present the minima for lamellar growth and the minima for rod-like growth intersect each other at the threshold growth rate equal to v = 400 μm/s. However, the minimization of entropy production does not yield information about the operating range for lamella➔rod transformation situated between threshold rate for transformation, v = 400 μm/s and final rate for transformation, v = 700 μm/s. This results from the fact that the minimization of entropy production is dealing with the regular structure formation only.

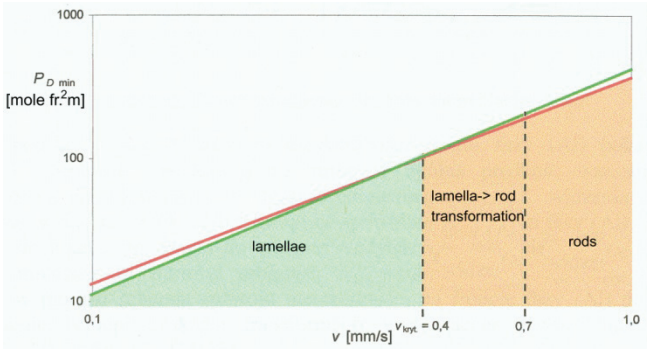

Figure 10. Entropy production minima calculated for the lamellar and rod-like structures formation at different solidification rates, typical for oriented growth of the Al-Si eutectic; the critical growth rate, $v_{kryt.}$ of the lamella ➔ rod transformation results from the trajectories intersection; it is equal to the threshold rate, v = 400 μm/s, once again.

A model of the evolution of the solid / liquid interface curvature versus the varying growth rate, v, Figure 11, with the resultant equilibrium at the triple point was used in the calculation of the minimum entropy production, Eq. (11). The above evolution results in crystallographic orientations evolution and confirms the specific surface free energies anisotropy.

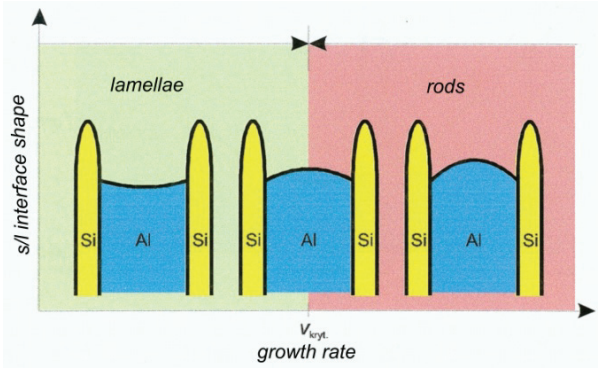

Figure 11. A model of the solid / liquid interface shape evolution with growth rate; it involves adequate changes of the crystallographic orientation of the s/l interface and finally changes of specific surface free energies and boundary free energy, Figure 12.

The varying values of the specific surface free energy, $\sigma_{Si}^{L} \equiv \sigma_{\beta}$, and boundary free energy, $\sigma_{Al-Si}^{L} \equiv \sigma_{\beta}$, as a function of the growth rate, v, for the lamellar structure formation are shown in Figure 12. The specific surface free energy $\sigma_{Al}^{L} \equiv \sigma_{\alpha}$ is to be calculated from the equilibrium, Eq. (7a). The rod-like structure energies were found analogously.

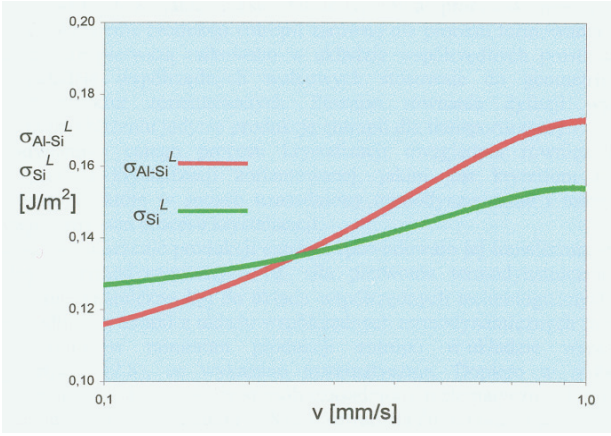

Figure 12. Postulated changes of the specific free energy and boundary free energy versus solidification rate, v; changes were selected to calculate trajectories of lamellar structure growth shown in Figure 7 and Figure 10.

As the threshold rate of growth was determined only, Figure 10, the growth of branches is to be analyzed. It allows to develop a complex theory for the formation of the irregular/regular eutectic morphology. It will also enable to explain why the operating range, Figure 10, appears.

It is postulated that the maximum destabilization of the solid/liquid interface of the non-faceted phase is observed just when the branching begins, Figure 13. The branches decrease the inter-lamellar spacing (this is required by the diffusion). The diminishing of spacing occurs until minimal distance between lamellae is reached. The minimal distance corresponds to regular structure formation in steady-state according to the criterion of minimum entropy production.

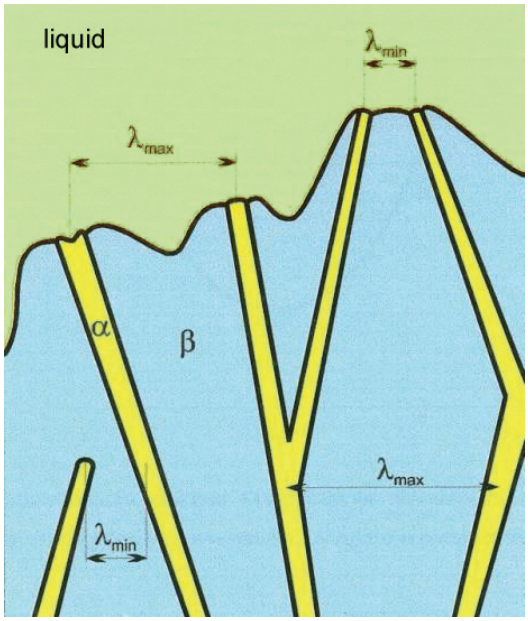

Figure 13. Phenomenon of branching as observed within the Al-Si eutectic structure; λ_{min} represents the area where locally the regular structure is formed; λ_{max} represents the area where branching appears and maximal instability of the solid / liquid interface of the Al - non-faceted phase is visible, Fisher and Kurz (1980).

The wave of perturbation is created at this destabilized s/l interface, Figure 14. It is assumed that the wavelength of maximum destabilization can be referred to as marginal stability. When a perturbation develops then the local

growth rate of the non-faceted phase decreases. Thus, the lamellae appear locally at the same time when rods are formed.

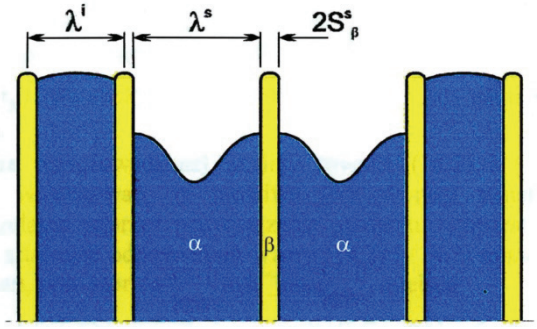

Figure 14. Creation of the maximal perturbation wave at the solid /liquid interface of the Al - non-faceted phase just before a branching which begins from the Si - faceted phase, $\beta \equiv Si - phase; \alpha \equiv Al - phase;\ S_\beta^S \equiv S_{Si}$; (non-coupled growth of this Si-lamella, which results in the important protrusion); λ^i - the minimal inter-lamellar spacing connected with the steady-state and criterion of the minimum entropy production; λ^S - the maximal inter-lamellar spacing connected with the maximal destabilization of the Al - solid/liquid interface and marginal stability.

When a perturbation vanishes then the local growth rate increases and reaches the growth rate proper for regular structure formation, locally. In this area a rod-like structure is the stable form within the operating range.

As a consequence of branching, the oscillation of the inter-phase spacing also occurs, Figure 15.

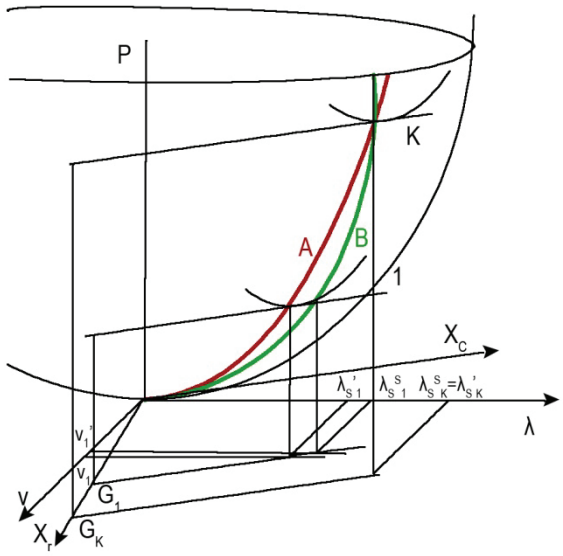

Figure 15. *Visualization of both: A - trajectory of local minima of the entropy production, B - trajectory of the marginal stability (excess entropy production tends to zero at this trajectory); two coordinate systems are visible: the thermodynamic system (X_C, X_T) and technological system (v, λ); $X_T \equiv G$; at a given state denoted "1" oscillation occurs between trajectory **A** and **B** as shown schematically; in this state two structural distances are formed within the eutectic morphology: inter-lamellar spacing $\lambda_{S1}^S(v_1')$ which corresponds to marginal stability, and inter-lamellar spacing $\lambda_{S1}'(v_1)$ which corresponds to minimum entropy production, with $v_1' < v_1$;*

When $\lambda_{SK}^S = \lambda_{SK}'$, the critical thermodynamic force is to be applied, that is the critical thermal gradient , G_K, Figure 15. In this case both trajectories intersect each other and oscillation vanishes.

Technologically, it means that the irregular structure transforms completely into a regular one and the marginal stability reduces to the minimum entropy production (point K), Figure 15.

The same reduction is observed when solidification rate tends to zero, Figure 15.

The oscillation of the inter-phase spacing can be generalized to the oscillation of the whole eutectic system between local minimum of entropy production (an attractor denoted as A) and an adequate state of marginal stability (bifurcation point for branching denoted as B), for a given condition of growth, $v, G = const.$, Figure 16.

The discussed oscillation justifies fully the appearance of the operating range (defined experimentally, Figure 10). In fact, locally, the growth rate diminishes (due to the creation of marginal stability) and the lamellae are in a stable form while in a neighboring area the growth rate is sufficiently greater to ensure the formation of rods, Figure 3b.

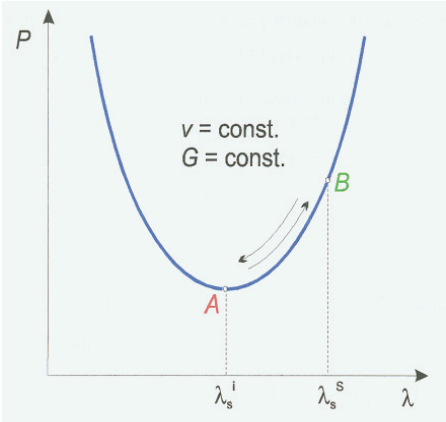

Figure 16. *Oscillation of the eutectic system between the steady-state defined by an A - attractor (local minimum of entropy production created for a given growth rate, v, and temperature gradient, G) and a B - marginal stability defined by an excess entropy production equal to zero (B can be treated as the bifurcation point for which a branching occurs together with the creation of maximal instability wave); λ_S^i is the inter-lamellar spacing connected with the attractor; λ_S^S is the inter-lamellar spacing referred to the branching (bifurcation); P - entropy production.*

The transformation of the irregular structure into completely regular structure (when oscillation vanishes - point K, Figure 15) was observed experimentally within the Al-Si eutectic system, Major and Rutter (1989).

When the oscillation vanishes the operating range for transformation, Figure 10, reduces to the threshold rate for transformation because the fully coupled growth of both the wetting Al - non-faceted phase and the Si – faceted phase is to be observed. Thus, in this case, the characterization of the lamella ➔ rod transformation by means of the calculation of the *Gibbs'* free energy is sufficient, Figure 7.

The complete transformation of the irregular structure into the regular structure (with no branches) can also be

performed experimentally when the applied growth rate would be equal to zero, Figure 15.

4. Concluding remarks

Two descriptions of the Al-Si eutectic solidification are given within the current analysis:
a/ associated with the thermodynamics of the solid / liquid interface formation and
b/ associated with the thermodynamics of the whole solidification process.

It allows to explain the lamella ➔ rod transformation together with the irregular structure ➔ regular structure transformation.

The appearance of the so-called operating range for lamella ➔ rod transformation together with the threshold rate for transformation are described thermodynamically by entropy production and critical perturbation of an interface.

The oscillation of the eutectic system between an attractor defined by the minimum entropy production and marginal stability, is introduced into the analysis, Figure 15.

The structural oscillation of the inter-phase spacing is justified by the creation of two thermodynamic states: the steady-state and the marginal stability state. Both states are visualized on a paraboloid of the entropy production, (drawn schematically in the function of two thermodynamic forces: X_C, X_T) Figure 15.

The provided theory has a general meaning and can be applied not only to the Al-Si eutectic system but to other eutectic systems which manifest the lamella ➔ rod transformation, for example: Al-Al_2Cu, Fe-Fe_3C, Fe-C or Zn-$Zn_{16}Ti$.

The applied criterion of the minimum entropy production, Eq. (11) allows the determination of the so-called growth law for both types of the regular structure:
$2\,W_5\,v^2\left(S_\alpha+S_\beta\right)^4+W_4\,v\left(S_\alpha+S_\beta\right)^3-W_1\left(S_\alpha+S_\beta\right)=2\,W_2$, for the lamellar structure formation and analogously $2\,V_5\,v^2\left(r_\alpha+r_\beta\right)^4+V_4\,v\left(r_\alpha+r_\beta\right)^3-V_1\left(r_\alpha+r_\beta\right)=2\,V_2$ for the rod-like structure formation.

According to above growth laws, one and only one inter-phase spacing, $\lambda,\ R$, can be selected in a given eutectic system solidifying at the imposed control parameters: $v,\ G$ and with some material parameters of this regular eutectic.

The marginal state created locally in an irregular eutectic results in the selection of the other inter-phase spacing equal to the perturbation wavelength which destabilizes the solid / liquid interface of the non-faceted phase.

The definition of this wavelength can be formulated as follows: $\lambda_s^S=2\,\pi\,\{\Gamma_\alpha/[|m_\alpha|(-v/D)(1-k_\alpha)\,N_E^L-G]\}^{0.5}$.

Usually, an average inter-phase spacing should be known to characterize a given generally irregular eutectic structure: $\bar{\lambda}=f(\lambda,\lambda_s^S)$ or $\bar{R}=f(R,\lambda_s^S)$ with Eq. (5).

The eutectic transformation occurs in the stationary / marginal state in such a way that lamellae / rods of the irregular structure formed at the imposed constant thermal gradient, G, and at the imposed constant solidification rate, v, manifest an average inter-phase spacing coming from the λ, R - parameters connected with the minimum entropy production and from the λ_S^i - parameter referred to the wavelength of the solid/liquid interface perturbation.

Acknowledgements

The financial support from the Polish Ministry of Science and Higher Education (MNiSW) under the contract N N508 480038 is gratefully acknowledged.

Nomenclature

a^L capillarity parameter used by Jackson and Hunt (1966)
a^R capillarity parameter used by Jackson and Hunt (1966)
D diffusion coefficient, [m^2/s]
E s/l interface geometry parameter, Cupryś et al. (2000)
G thermal gradient at the s/l interface, [K/m]
k_α partition ratio for the α – phase, [mole fr./mole fr.]
L_α heat of fusion per unit volume of the α - phase, [J/m^3]
L_β heat of fusion per unit volume of the β - phase, [J/m^3]
m_α slope of the α – liquidus line, [K/mole fr.]
m_β slope of the β – liquidus line, [K/mole fr.]
N_i concentration of the i-th solute in the liquid, [mole fr.]
N_0 difference of the Si – solute solubility in the α-eutectic phase and β-eutectic phase, [mole fr.]
N_E^L Si – solute eutectic concentration, [mole fr.],
P_D total entropy production associated with mass transfer, [mole $fr.^2$ /m]
$\bar{P}_D^L$ average total entropy production associated with mass transfer for lamellar growth, [mole $fr.^2$/m]
$\bar{P}_D^R$ average total entropy production associated with mass transfer for rod-like growth, [mole $fr.^2$/m],
P^* s/l interface geometry parameter, Cupryś et al. (2000),
Q^L s/l interface geometry parameter defined by Jackson and Hunt (1966) for lamellar structure formation,
Q^R s/l interface geometry parameter defined by Jackson and Hunt (1966) for rod-like structure formation
R^* gaze constant, [J/(mole fr. K)]
r_α rod radius, Figure 9b
r_β thickness of the matrix collar, Figure 9b
$\bar{R}$ average inter-rod spacing within the generally irregular structure, [m]
S_α half the width of the α – phase lamella, [m], Figure 9a
S_β half the width of the β – phase lamella, [m], Figure 9a
T_E eutectic temperature, [K]
V volume used in the integrals, Figure 8, [m^3]
v growth rate imposed in directional solidification, [m/s]
V_i coefficients containing material parameters defined by Cupryś et al. (2000), for rod-like structure; $i=1,\ldots,5$
W_i coefficients containing material parameters defined by Cupryś et al. (2000), for lamellar structure; $i=1,\ldots,5$
α eutectic phase, usually the non-faceted phase
β eutectic phase, usually faceted phase
Γ_α *Gibbs-Thompson* capillarity parameter, [K m]
ΔT_L^* solid/liquid interface undercooling for the lamellar structure formation, [K]
ΔT_R^* solid/liquid interface undercooling for the rod-like structure formation, [K]
ΔG_L^* *Gibbs'* free energy of the s/l interface for the lamellar structure formation, [J/m^3]
ε thermodynamic constant
θ_S^L angle between tangent to the s/l interface and x – axis at the triple point, for lamellar structure, $S=\alpha,\beta$, [^{0}]
θ_R^L angle between tangent to the s/l interface and x – axis at the triple point, for rod-like structure, $S=\alpha,\beta$, [^{0}]
θ_S angle between tangent to the s/l interface and x – axis at the triple point, generally for lamellar and rod-like structures, Figure 5, [^{0}]

λ inter-lamellar spacing for regular structure, Figure 4a, adapted to define an irregular structure through λ^i, Figure 14 or through λ_{min}, Figure 13, and to an oscillation system as λ_s^i; $\lambda \equiv \lambda^i \equiv \lambda_s^i \equiv \lambda_{min}$, [m]

λ_s^S maximal wavelength of perturbation at the s/l interface, also visible in an oscillation system, Figure 16, and within an irregular structure as λ^s, Figure 14, or as λ_{max}, Figure 13, $\lambda_s^S \equiv \lambda^s \equiv \lambda_{max}$, [m]

$\bar{\lambda}$ average inter-lamellar spacing within the generally irregular structure, [m]

σ_S specific surface free energy, generally for lamellar and rod-like structures, Figure 5, $S = \alpha, \beta$, [J/m^2]

σ_S^L specific surface free energy, particularly for lamellar structure, $S = \alpha, \beta$, [J/m^2]

σ_S^R specific surface free energy, particularly for rod-like structure, $S = \alpha, \beta$, [J/m^2]

$\sigma_{\alpha-\beta}$ phase boundary free energy, generally for lamellar and rod-like structure, [J/m^2]

$\sigma_{\alpha-\beta}^L$ phase boundary free energy, particularly for lamellar structure, [J/m^2]

$\sigma_{\alpha-\beta}^R$ phase boundary free energy, particularly for rod-like structure, [J/m^2]

Appendix

Additionally, some definitions are given below to explain the meaning of the symbols used in the text:

$a_S^L = (T_E/L_S)\, \sigma_S^L \, \sin\theta_S^L$ with $L_S = L_\alpha, L_\beta$

$a_S^R = (T_E/L_S)\, \sigma_S^R \, \sin\theta_S^R$ with $L_S = L_\alpha, L_\beta$

$1/m = 1/m_\alpha + 1/m_\beta$

$z = g(x)$ is the hypothetical function which is able to describe the shape of the solid / liquid interface and its curvature, Figure 8a.

References

Atasoy, O., 1984, "Effects of Unidirectional Solidification Rate and Composition on Inter-particle Spacing in Al-Si Eutectic Alloy", *Aluminium*, Vol. 60, pp.109-116.

Cupryś, R., Major, B., Wołczyński, W., 2000, "Transition of Flake into Fibre Structure in Eutectic Al-Si" , *Materials Science Forum*, Vol. 329/330, pp.161-166.

Elliott, R., 1977, "Eutectic Solidification", *International Metals Reviews,* Vol. 219, pp. 161-186.

Fisher, D.J., Kurz, W., 1980, "A Theory of Branching Limited Growth of Irregular Eutectics", *Acta Metallurgica*, Vol. 28, pp. 777-794.

Glansdorff, P., Prigogine, I., 1971, *Thermodynamic Theory of Structure, Stability and Fluctuations*, John Wiley & Sons, Ltd. London-New York – Sydney- Toronto.

Jackson, K.A., Hunt, J.D., 1966, "Lamellar and Rod Eutectic Growth", *Transactions of the AIME*, Vol. 236, pp. 1129-1142.

Lesoult, G., Turpin, M., 1969, "Etude theorique sur la croissance des eutectiques lamellaires", *Revue Scientifique de Metallurgie,* Vol. 9, pp. 619-631.

Major, J.F., Rutter, J.W., 1989, "Effect of Strontium and Phosphorus on Solid/Liquid Interface of Al-Si Eutectic", *Materials Science and Technology*, Vol. 5, pp. 645-656.

Steen, H.A.H., Hellawell, A., 1975, " The Growth of Eutectic Silicon – Contributions to Undercooling", *Acta Metallurgica,* Vol. 23, pp. 529-536.

Toloui, B., Hellawell, A., 1976, "Phase Separation and Undercooling in Al-Si Eutectic Alloy – The Influence of Freezing Rate and Temperature Gradient", *Acta Metallurgica*, Vol. 24, pp. 565-572.

Wołczyński, W., Billia, B., 1996, "Influence of Control and Material Parameters on Regular Eutectic Growth and Inter-lamellar Spacing Selection", *Materials Science Forum*, Vol. 215/216, pp.313-322.